DYNAMIC ANALYSIS OF THE THREE-PHASE DC/DC CONVERTER WITH ASYMMETRICAL DUTY CYCLE, ASSOCIATED TO A THREE-PHASE VERSION OF THE HYBRIDGE RECTIFIER

Demercil S. Oliveira Jr., Ivo Barbi
Institute of Power Electronics – INEP
Federal University of Santa Catarina – UFSC
demercil@inep.ufsc.br, ivobarbi@inep.ufsc.br

***Abstract* – This paper presents the theoretical analysis concerning the operating stages of the three-phase dc/dc converter associated to the hybridge rectifier, in order to obtain its dynamic model. The dynamic model, the controller design, as well as the experimental results obtained from a prototype of 6kW are presented.**

KEYWORDS

Three-phase dc/dc converter, hybridge rectifier, asymmetrical duty cycle.

I. INTRODUCTION

Nowadays, the main topology used in high power dc/dc conversion is the ZVS PWM Full Bridge converter [1][2]. It is characterized by four switches operating in high frequency. The soft commutation can be obtained by using phase shift modulation, which preserves the simplicity and achieves high power density.

However, for higher power levels, the components face several stresses. As possible solutions, the parallelism of components or even converters can be applied. The former choice increases the complexity of the compromise between the layout circuit and the thermal design. Besides that, one should consider that the dynamic and static current sharing problem limits its application. The other alternative causes redundancy in the control circuits as well as in the number of power components and drivers, increasing the global cost and size of the equipment.

A prominent alternative was proposed by Ziogas [3]. It uses a three-phase inverter coupled to a three-phase high frequency transformer and to a three-phase high frequency rectifier. The resulting advantages consist in the increase of the input and output current frequency, by a factor of three compared to the Full Bridge converter, lower rms current through power components and reduction of the cores.

Although it presents satisfactory advantages, soft commutation has not been achieved, which limits the switching frequency and the power density. Then, the use of the asymmetrical duty cycle [4] in the three-phase dc/dc converter was proposed [5], in order to provide the ZVS commutation of all switches for a wide load range. Nevertheless, the resulting topology suffers high conduction losses, since two series diodes conduct the load current.

Therefore it was stated in [6] that the use of the three-phase version of the hybridge rectifier, associated to the three-phase dc/dc converter with asymmetrical duty cycle, improves the efficiency obtained with the same converter associated to the six-diode rectifier. Within this context, this paper fulfills the theoretical development of the proposed converter, focusing on its dynamic behavior.

II. DYNAMIC ANALYSIS

The circuit of the three-phase dc/dc converter associated to the hybridge rectifier is shown in Fig. 1. According to the operating stages described in [6], one can obtain the state space equations for each operating stage, as the following assumptions are established:

- All semiconductors are ideal;
- All parasitic components are neglected, except for the series resistance of the output capacitor.

In addition, the state-space variables are the output current $i_T=i_{L1}+i_{L2}+i_{L3}$ and the voltage on the capacitor v_C.

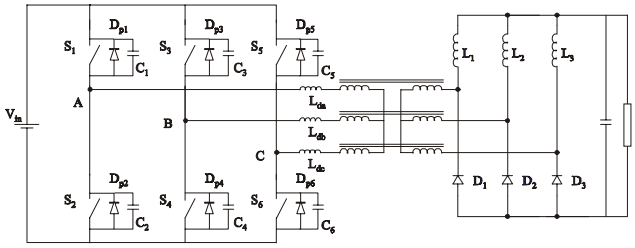

Fig. 1 – Three-phase ZVS dc/dc converter with the hybridge rectifier.

A. Mode DMIN

From the operating stages description [6], one can obtain the state space equation (1), valid for this mode, where $L=L_1/3$.

$$\begin{bmatrix} \dot{i}_L \\ \dot{v}_C \end{bmatrix} = \begin{bmatrix} -\frac{1}{L}\cdot\frac{R\cdot r_{SE}}{R+r_{SE}} & -\frac{1}{L}\cdot\frac{R}{R+r_{SE}} \\ \frac{1}{C}\cdot\frac{R}{R+r_{SE}} & -\frac{1}{C}\cdot\frac{1}{R+r_{SE}} \end{bmatrix} \begin{bmatrix} i_L \\ v_C \end{bmatrix} + \begin{bmatrix} \frac{1+3q(t)}{6L} \\ 0 \end{bmatrix} V_{in} \quad (1)$$

Where the switching function q(t) is defined as follows:

$$q(t) = \begin{cases} 1, \text{ if stage 2} \\ 0, \text{ if stage 1 or 3} \end{cases} \quad (2)$$

The equilibrium points are given by (3), and the eigenvalues can be real or complex, depending on the parameters of the circuit.

$$\bar{X} = \begin{bmatrix} \frac{1}{3R} \\ \frac{1}{3} \end{bmatrix} V_{in} q(t) \quad (3)$$

Defining the average effective duty cycle in (4), where *Rd* is the duty cycle loss caused by the series inductance $L_d=L_{da}=L_{db}=L_{dc}$, the nonlinear model, in the average state space, can be obtained in (6).

$$d = D_{ef}(t) = \langle q(t) \rangle_{T_s} - \frac{R_d}{V_{in}} \langle i_L(t) \rangle_{T_s} \tag{4}$$

$$R_d = f_s L_d \tag{5}$$

$$\begin{bmatrix} \dot{i}_L \\ \dot{v}_C \end{bmatrix} = \begin{bmatrix} -\frac{1}{L} \cdot \frac{R \cdot r_{SE}}{R + r_{SE}} & -\frac{1}{L} \cdot \frac{R}{R + r_{SE}} \\ \frac{1}{C} \cdot \frac{R}{R + r_{SE}} & -\frac{1}{C} \cdot \frac{1}{R + r_{SE}} \end{bmatrix} \begin{bmatrix} i_L \\ v_C \end{bmatrix} + \begin{bmatrix} \frac{d}{L} \\ 0 \end{bmatrix} V_{in} \tag{6}$$

By equaling its derivative to zero, the equilibrium points of the nonlinear model can be obtained.

$$\bar{X} = \begin{bmatrix} \frac{1}{R + R_d} \\ \frac{R}{R + R_d} \end{bmatrix} d \cdot V_{in} \tag{7}$$

B. Mode DMED

From the operating stages description [6], one can obtain the state space equation (8), valid for this mode, where $L=L_1/3$.

$$\begin{bmatrix} \dot{i}_L \\ \dot{v}_C \end{bmatrix} = \begin{bmatrix} -\frac{1}{L} \cdot \frac{R \cdot r_{SE}}{R + r_{SE}} & -\frac{1}{L} \cdot \frac{R}{R + r_{SE}} \\ \frac{1}{C} \cdot \frac{R}{R + r_{SE}} & -\frac{1}{C} \cdot \frac{1}{R + r_{SE}} \end{bmatrix} \begin{bmatrix} i_L \\ v_C \end{bmatrix} + \begin{bmatrix} \frac{1 + 3q(t)}{6L} \\ 0 \end{bmatrix} V_{in} \tag{8}$$

Where the switching function q(t) is defined as follows:

$$q(t) = \begin{cases} 1, \text{ if stage 1} \\ 0, \text{ if stage 2 or 3} \end{cases} \tag{9}$$

The equilibrium points are given by (10), and the eigenvalues can be real or complex, depending on the parameters of the circuit.

$$\bar{X} = \begin{bmatrix} \frac{V_{in}(1 + 3q(t))}{6R} \\ \frac{V_{in}(1 + 3q(t))}{6} \end{bmatrix} \tag{10}$$

Using the average effective duty cycle (4), where *Rd* is the duty cycle loss caused by the series inductance $L_d=L_{da}=L_{db}=L_{dc}$, the nonlinear model, in the average state space, can be obtained (12).

$$R_d = 3 f_s L_d \tag{11}$$

$$\begin{bmatrix} \dot{i}_L \\ \dot{v}_C \end{bmatrix} = \begin{bmatrix} -\frac{1}{L} \cdot \frac{R \cdot r_{SE}}{R + r_{SE}} & -\frac{1}{L} \cdot \frac{R}{R + r_{SE}} \\ \frac{1}{C} \cdot \frac{R}{R + r_{SE}} & -\frac{1}{C} \cdot \frac{1}{R + r_{SE}} \end{bmatrix} \begin{bmatrix} i_L \\ v_C \end{bmatrix} + \begin{bmatrix} \frac{d}{L} \\ 0 \end{bmatrix} V_{in} \tag{12}$$

By equaling its derivative to zero, the equilibrium points of the nonlinear model can be obtained.

$$\bar{X} = \begin{bmatrix} \frac{1}{R + R_d} \\ \frac{R}{R + R_d} \end{bmatrix} d \cdot V_{in} \tag{13}$$

C. Mode DMAX

From the operating stages description [6], one can obtain the state space equation (14), valid for this mode, where $L=L_1/3$.

$$\begin{bmatrix} \dot{i}_L \\ \dot{v}_C \end{bmatrix} = \begin{bmatrix} -\frac{1}{L} \cdot \frac{R \cdot r_{SE}}{R + r_{SE}} & -\frac{1}{L} \cdot \frac{R}{R + r_{SE}} \\ \frac{1}{C} \cdot \frac{R}{R + r_{SE}} & -\frac{1}{C} \cdot \frac{1}{R + r_{SE}} \end{bmatrix} \begin{bmatrix} i_L \\ v_C \end{bmatrix} + \begin{bmatrix} \frac{q(t)}{1.5L} \\ 0 \end{bmatrix} V_{in} \tag{14}$$

Where the switching function q(t) is defined as follows:

$$q(t) = \begin{cases} 0, \text{ if stage 1} \\ 1/4, \text{ if stage 2} \\ 1, \text{ if stage 3} \end{cases} \tag{15}$$

The equilibrium points are given by (3), and the eigenvalues can be real or complex, depending on the circuit parameters.

$$\bar{X} = \begin{bmatrix} \frac{2}{3R} \\ \frac{2}{3} \end{bmatrix} V_{in} q(t) \tag{16}$$

Using the average effective duty cycle in (4), where *Rd* is the duty cycle loss caused by the series inductance $L_d=L_{da}=L_{db}=L_{dc}$, the nonlinear model, in the average state space, can be obtained in (6).

$$R_d = 3 f_s L_d \tag{17}$$

$$\begin{bmatrix} \dot{i}_L \\ \dot{v}_C \end{bmatrix} = \begin{bmatrix} -\frac{1}{L} \cdot \frac{R \cdot r_{SE}}{R + r_{SE}} & -\frac{1}{L} \cdot \frac{R}{R + r_{SE}} \\ \frac{1}{C} \cdot \frac{R}{R + r_{SE}} & -\frac{1}{C} \cdot \frac{1}{R + r_{SE}} \end{bmatrix} \begin{bmatrix} i_L \\ v_C \end{bmatrix} + \begin{bmatrix} \frac{q(t)}{1.5L} \\ 0 \end{bmatrix} V_{in} \tag{18}$$

By equaling its derivative to zero, the equilibrium points of the nonlinear model can be obtained.

$$\bar{X} = \begin{bmatrix} \frac{2}{3R} \\ \frac{2}{3} \end{bmatrix} q(t) \cdot V_{in} \tag{19}$$

Using the average effective duty cycle (4), where *Rd* is the duty cycle loss caused by the series inductance $L_d=L_{da}=L_{db}=L_{dc}$, the nonlinear model, in the average state space, can be obtained (21).

$$R_d = 3 f_s L_d \tag{20}$$

$$\begin{bmatrix} \dot{i}_L \\ \dot{v}_C \end{bmatrix} = \begin{bmatrix} -\frac{1}{L} \cdot \frac{R \cdot r_{SE}}{R + r_{SE}} & -\frac{1}{L} \cdot \frac{R}{R + r_{SE}} \\ \frac{1}{C} \cdot \frac{R}{R + r_{SE}} & -\frac{1}{C} \cdot \frac{1}{R + r_{SE}} \end{bmatrix} \begin{bmatrix} i_L \\ v_C \end{bmatrix} + \begin{bmatrix} \frac{d}{L} \\ 0 \end{bmatrix} V_{in} \tag{21}$$

By equaling its derivative to zero, the equilibrium points of the nonlinear average model can be obtained.

$$\bar{X} = \begin{bmatrix} \frac{1}{R + R_d} \\ \frac{R}{R + R_d} \end{bmatrix} 2(1 - d) \cdot V_{in} \tag{22}$$

D. Linearization

Defining the equilibrium points (I_L, V_C, D, V_{in}, R), and using the Jacobian concept, the linearized average state space equation can be found.

$$\begin{bmatrix} \dot{i}_L \\ \dot{v}_C \end{bmatrix} = \begin{bmatrix} -\frac{1}{L}\cdot\frac{R\cdot r_{SE}}{R+r_{SE}} & -\frac{1}{L}\cdot\frac{R}{R+r_{SE}} \\ \frac{1}{C}\cdot\frac{R}{R+r_{SE}} & -\frac{1}{C}\cdot\frac{1}{R+r_{SE}} \end{bmatrix} \begin{bmatrix} i_L \\ v_C \end{bmatrix} + \begin{bmatrix} \frac{V_{in}}{L} & \frac{D}{L} & \frac{-dV_{in}r_{SE}}{(R+r_{SE})(R+r_{SE})} \\ 0 & 0 & \frac{dV_{in}}{(R+r_{SE})(R+r_{SE})} \end{bmatrix} \cdot \begin{bmatrix} \Delta d \\ \Delta v_{in} \\ \Delta r \end{bmatrix} \quad (23)$$

Solving the transference matrix, one can obtain the complete dynamic transfer functions of the three-phase dc/dc converter operating in the DMIN mode.

$$\frac{di_L}{dd} = \frac{V_{in}}{R}\frac{(r_{SE}+R)C\cdot s+1}{den(s)} \quad (24)$$

$$\frac{di_L}{dv_{in}} = \frac{D}{R}\frac{(r_{SE}+R)C\cdot s+1}{den(s)} \quad (25)$$

$$\frac{di_L}{dr} = -D\frac{V_{in}}{R(R+R_d)}\frac{r_{SE}C\cdot s+1}{den(s)} \quad (26)$$

$$\frac{dv_0}{dd} = V_{in}\frac{r_{SE}C\cdot s+1}{den(s)} \quad (27)$$

$$\frac{dv_0}{dv_{in}} = D\frac{r_{SE}C\cdot s+1}{den(s)} \quad (28)$$

$$\frac{dv_0}{dr} = -DV_{in}\frac{(L-r_{SE}{}^2C)\cdot s+R_d-r_{SE}}{(R+R_d)(R+r_{SE})den(s)} \quad (29)$$

Where:

$$den(s) = \begin{bmatrix} LC\left(\frac{r_{SE}}{R}+1\right)s^2 + \left[r_{SE}+R_d\left(\frac{r_{SE}}{R}+1\right)C+\frac{L}{R}\right]s \\ +\frac{R_d}{R}+1 \end{bmatrix} \quad (30)$$

Following the same procedure used in mode DMED, one can obtain the same equations presented previously (24)-(30), except for the R_d value. Hence, a unified equation was derived for the converter operating in modes DMIN and DMED.

$$R_d = \begin{cases} f_s L_d & \text{if DMIN} \\ 3f_s L_d & \text{if DMED} \end{cases} \quad (31)$$

For mode DMAX, the same procedure can be used, but the obtained equations can not be described in a unified way.

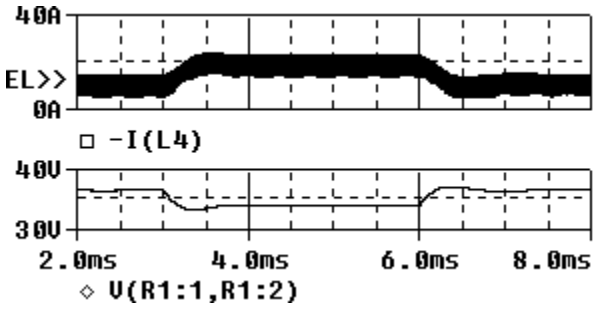

Fig. 2 – Load step response in the pspice.

E. Model Validation

In order to prove the validity of the developed nonlinear model, some simulation tests were performed. Fig. 2 and Fig. 3 show the dynamic responses obtained by PSPICE and by the nonlinear average model, under the same conditions and for the same load step. One can see that the obtained responses are almost the same, validating the accuracy of the developed model.

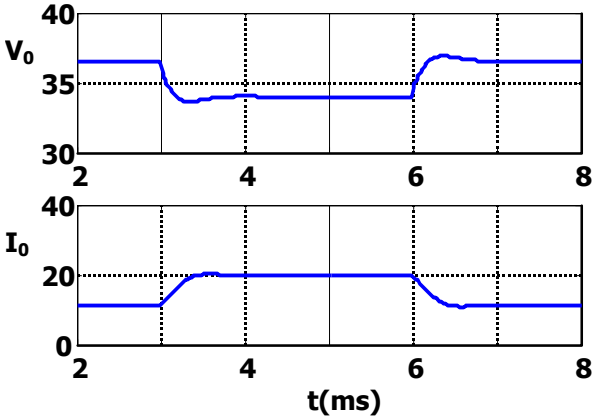

Fig. 3 – Load step response in the nonlinear average state space.

III. CONTROLLER DESIGN

As it can be seen, the resulting linearized model is analogous to the expressions of the Buck converter. Then, a similar controller can be used. Fig. 4 shows the Bode diagram of the system, in modes DMIN and DMED, where there is a small variation in the curves. Therefore only one controller can be used to control the system in regions 1 and 2. The systems parameters used to obtain such results are presented in TABLE 1.

TABLE 1
Parameters used in the prototype.

V_{IN}	n	P_0	L_D	L_F	T_S	R_0
420V	3.67	6kW	10µH	45µH	21.6µs	0.6Ω

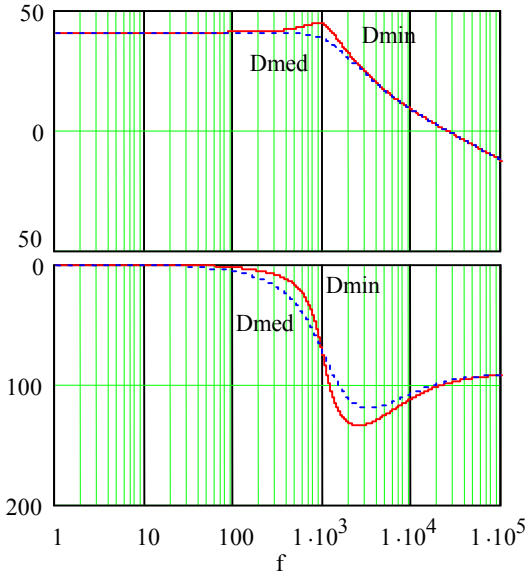

Fig. 4 – System response.

In order to maintain the output voltage constant under load variations, the following controller was designed:

$$G_c(s) = \frac{\left(1+\frac{s}{\omega_1}\right)^2}{\left(1+\frac{s}{\omega_G}\right)\left(1+\frac{s}{\omega_{za}}\right)} \qquad (32)$$

Where ω_1 is slightly smaller than ω_0 (natural resonant frequency of the system), ω_{za} is the frequency of the zero generated by r_{SE}, and ω_G the pole frequency needed to obtain the required crossover frequency (f_c). TABLE 2 shows the parameters values of the controller.

TABLE 2
Controller parameters.

f_C	ω_0	ω_{ZA}	ω_G	Q
$10*10^3$	$4.5*10^3$	$41.6*10^3$	$2.68*10^3$	0.745

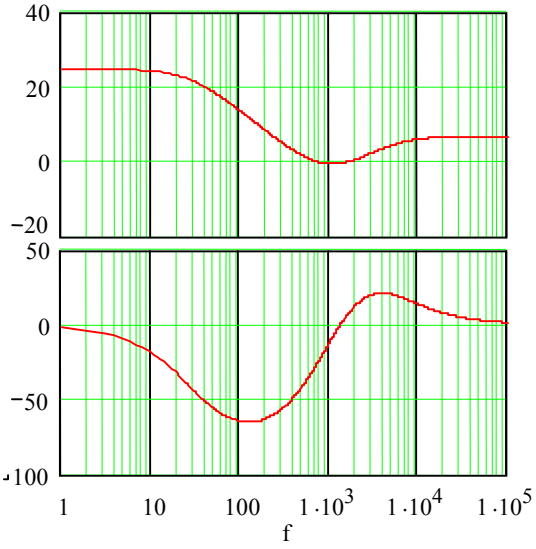

Fig. 5 – Controller response.

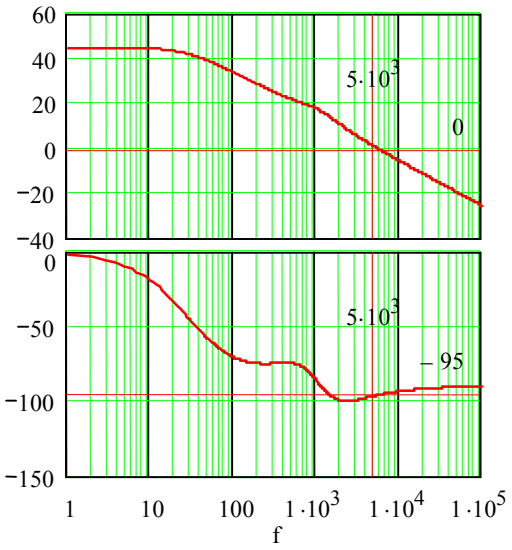

Fig. 6 – Open loop response.

IV. Experimental Results

Using the experimental prototype developed with the parameters presented in TABLE 1, some results were obtained in order to verify the closed loop response of the converter.

Fig. 7 and Fig. 8 show the dynamic behavior of the output inductor current during a load step. As it can be seen, the dynamic response is satisfactory, since there is no overshoot and the transient time is short.

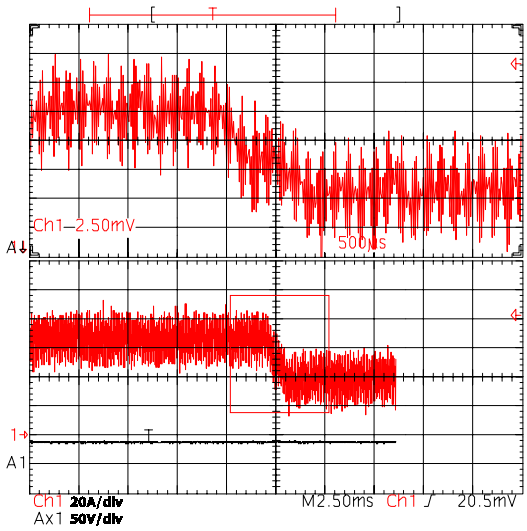

Fig. 7 – Closed loop system response (load current – 5A/div).

A comparison between the experimental results and those obtained with the developed nonlinear average model can be established, according to Fig. 9. As it can be seen, the experimental dynamic behavior of the output current corresponds to the simulation results.

The dynamic response of the output voltage could not be determined accurately, because its variation is very small, according to the simulation results shown in Fig. 10.

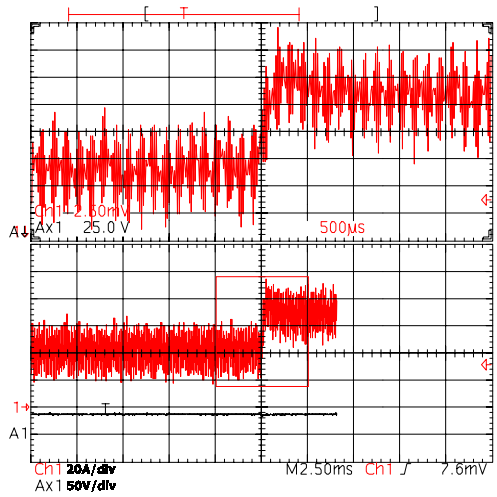

Fig. 8 – Closed loop system response (load current – 5A/div).

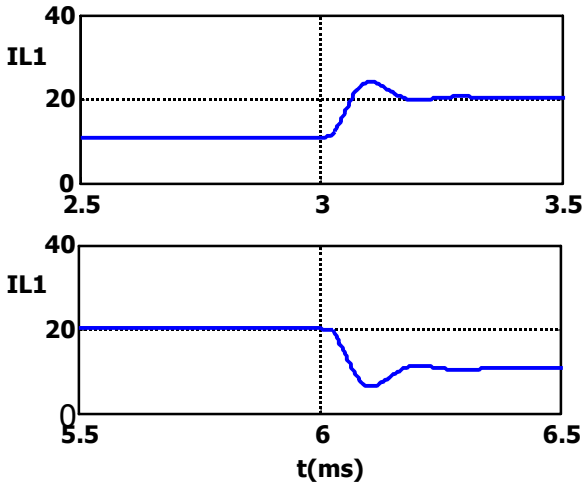

Fig. 9 – Closed loop system response obtained by simulation of the nonlinear average model (output current).

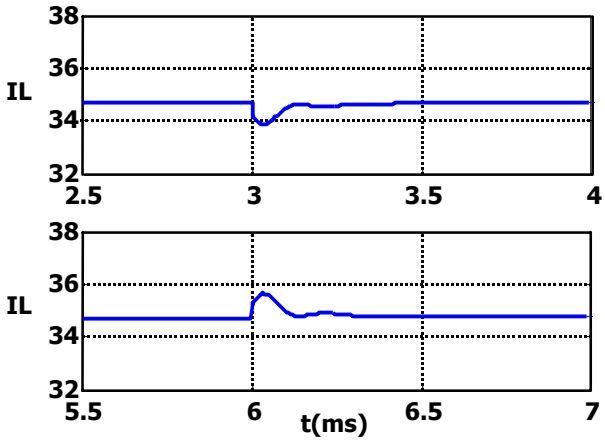

Fig. 10 – Closed loop system response obtained by simulation of the nonlinear average model (output voltage).

III. CONCLUSION

This paper has presented a dynamic analysis of the three-phase dc/dc converter with asymmetrical duty cycle. As expected, the obtained dynamic model is equivalent to the Buck converter model, although it includes some real characteristics as the presence of the leakage inductance and the use of three output inductors.

The developed model was studied by simulation and analysis of the step response under load variations. Then, a linearized model was obtained, in order to design a conventional controller.

Using a prototype of 6kW, some experimental closed loop responses were obtained. The experimental results have shown satisfactory agreement with the mathematical model, validating the adopted procedure design.

ACKNOWLEDGMENT

The authors acknowledge CAPES, CNPq and FEESC for the financial support to this work.

REFERENCES

[1] I. Barbi, W.A. Filho, “A Non-Resonant Zero Voltage Switching Pulse Width Modulated Full-Bridge DC/DC Converter,” in Proc. IECON 1990, pp 1051-1056.

[2] R.L. Steingerwald, K.D.T. Ngo, “Full-Bridge Lossless Switching Converter,” U.S. Patent 4864479, Sept 5, 1989.

[3] P.D. Ziogas, A.R. Prasad, S. Manias, “Analysis and design of a three phase off-line dc-dc converter with high frequency isolation,” IN Proc IAS 88, pp. 813 – 820

[4] N. Mohan, P. Imbertson, “Asymmetrical duty cycle permits zero switching loss in PWM circuits with no conduction loss penalty,” IEEE Transactions on Industry Applications, vol 29, no 1, jan/feb 1993, pp 121-125

[5] D.S. Oliveira Jr, I. Barbi, “A dc/dc ZVS three phase converter with asymmetrical duty cycle,” IN Proc. PESC 2003, Acapulco, Mexico

[6] D.S. Oliveira Jr, Ivo Barbi, “A Three-Phase Version Of The Hybridge Rectifier Associated To The Three Phase Dc/Dc Converter With Asymmetrical Duty Cycle,” in Proc. ISIE 2003, Rio de Janeiro, Brazil.